



DEVELOPMENT OF AIRFOILS BASED ON THEIR AERODYNAMIC CHARACTERISTICS USING ARTIFICIAL NEURAL NETWORKS

Bruno da Cunha Diniz

Raimundo Carlos Silverio Freire Júnior

Sandi Itamar Schafer de Souza

Universidade Federal do Rio Grande do Norte, Natal, RN - Brazil
dinizbc@gmail.com, freirej@gmail.com, sandi@ufrnet.br

Resumo. *One of the main concerns in Engineering nowadays is the development of aircrafts of low consumption and high performance. For this purpose, airfoils are studied and designed to have an elevated lift coefficient and a low drag coefficient, generating a highly efficient airfoil. The higher is the efficiency value, the lower will be the aircraft fuel consumption, thus improving its performance. In this sense, this work aims to develop a tool for airfoil creation from some desired characteristics, such as the lift and drag coefficients and maximum efficiency rate, using an algorithm based on an Artificial Neural Network (ANN). In order to do so, a database of aerodynamic characteristics with a total of 300 airfoils was initially collected from the XFOil software. Then, through a routine implemented in the MATLAB software, network architectures of one, two, three and four modules were trained, using the Backpropagation algorithm and Momentum. The cross-validation technique was applied to analyze the results, evaluating which network possesses the lowest value in root-mean-square error (RMS). In this case, the best result obtained was from the two-module architecture with two hidden neuron layers. The airfoils developed by this network, in the regions with the lowest RMS, were compared to the same airfoils imported to XFOil. The presented work offers as a contribution, in relation to other works involving ANN applied to fluid mechanics, the development of airfoils from their aerodynamic characteristics.*

Keywords: *Airfoils, aerodynamic characteristics, Artificial Neural Networks, network architectures.*

1. INTRODUCTION

One of the main concerns in the development of aerodynamic airfoils is efficiency. This variable, which corresponds to the ratio between aerodynamic force and drag (force contrary to the aircraft movement), is highly important to the aircraft performance. The higher is the efficiency value, the lower is the aircraft fuel consumption, although an increase in resistance commonly follows the increase in lift, nevertheless, it is still intended to project new airfoils to match these features.

Following this line of thought, there are many works in literature (Eppler, 1974; Truckenbrodt, 1951; Wortmann, 1961) applying techniques for airfoil design, and also among these techniques, artificial neural networks are used (Rai and Madavan, 2000). Ross *et al.* (1997) used artificial neural networks to minimize the amount of necessary data to completely define the aerodynamic performance of a model examined in a wind tunnel. In this case, the author experimentally used only 50% of the data, and achieved results with the trained neural network which were very close to the ones from the performed measurements. Wallach *et al.* (2006), Rajkumar and Bardina (2002, 2003) and Soltani *et al.* (2007) used other applications of the ANN in airfoils, in the prediction of aerodynamic coefficients of airfoils and aircrafts using artificial neural networks. Nørgaard *et al.* (1997) used ANN for more efficient design evaluations and in order to find ideal configurations for flaps. The author also used four networks to predict the C_L , C_D , C_M and L/D coefficients and one network to analyze the flap configurations. On the other hand, Maezabadi *et al.* (2008) analyzed the air draining in a section of a blade of a wind turbine, using the network to predict the behavior of the flow in the airfoil for the desired conditions.

Nowadays, there is a lot of software able to display the aerodynamic behavior of an airfoil from its geometry. Such methodology is opposed to the proposition of this work, which is to develop the airfoil (geometry) from some of its important aerodynamic attributes.

This work aims to develop airfoils from the desired characteristics (lift, drag and maximum efficiency rate), using an artificial neural network. Thereunto, an algorithm is used based on artificial neural networks with several different types of architecture. As specific goals, it stand out the evaluation of neural architectures presenting the lowest margin of error in relation to the airfoils used, and the development of new architectures based on committee machines (modular networks) aiming to improve results and become appropriate for the evaluated airfoils.

It is worth mentioning that the airfoils are not used exclusively for application in aircrafts, but may also present other uses, such as wind power generator blades, pumps, fans, etc.

2. METHODOLOGY

2.1 Data used on the training and testing of the ANN architectures

This stage of the process consisted in the conception of a database containing airfoils and some of their most important characteristics for the training of the neural network.

The necessary data for the training were collected in the **XFOIL** software (Drela and Youngren, 2001), which is engaged in the examination of airfoils. Starting with geometry and the Reynolds number, the software calculates the distribution of pressure and characteristics involving lift, drag and momentum submitted in the airfoil for different angles of attack.

The Reynolds number was established in 5×10^5 for every airfoil analyzed and, initially, the data were collected at random. The graph exhibited in Fig. 1(a) shows the distribution of the randomly collected data for one of the airfoil characteristics, the maximum efficiency rate. In order to obtain a better distribution in the values to be used in the ANN training, as from the second half of the data, the airfoils were collected intending to homogenize the input values of the ANN, avoiding a poor generalization during the training, as shown in Fig 1(b).

Besides the maximum efficiency rate (E_{fmax}), the following airfoil characteristics were collected: the lift coefficient (C_l), the drag coefficient (C_d) and the momentum coefficient (C_m), when the angle of attack of the airfoil equals zero. In addition, geometric coordinates in the vertical and horizontal axes were also used for all of the airfoils, in order to compose the output database of the training, thus obtaining a database with a total of 300 airfoils.

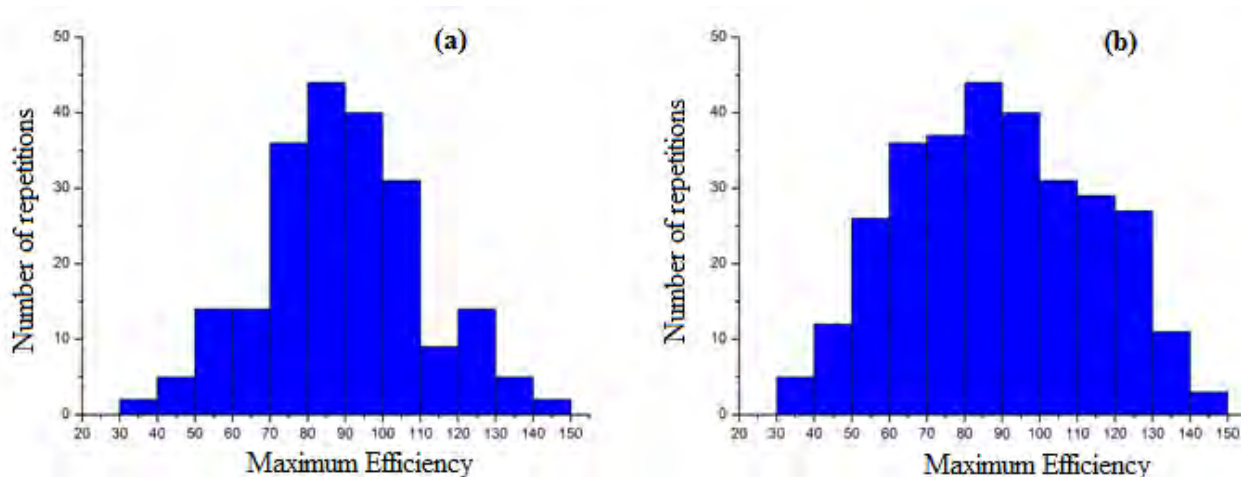


Figure 1. Histogram of the maximum efficiency rate values (a) before homogenization; (b) after homogenization of the database

2.2 Preprocessing of the database

At this stage, the database is randomly divided into an estimation database and a test database. The estimation database is also divided into two subsets: *training* (utilized to train the ANN) and *validation* (utilized to validate the ANN). Tab. 1 shows the results of airfoil distribution for each case.

Table 1. Division of the database

DATABASE	NUMBER OF DATA
Training set	240
Validation set	30
Test set	30

Aiming to standardize the airfoil geometric coordinates (position against a reference axis where zero is located at the beginning of the leading edge and the chord equals the unit in all airfoils) such coordinates were interpolated, ensuring standardization among the airfoils. An example of two airfoils and their interpolations is demonstrated in Fig. 2. It is also worth mentioning that after the interpolation, it was decided to use a larger number of points in the region between 0 and 0.25 of the abscissa (x axis), since most of the airfoils have a more complex geometry in this region (leading edge), thus enhancing the precision of the results.

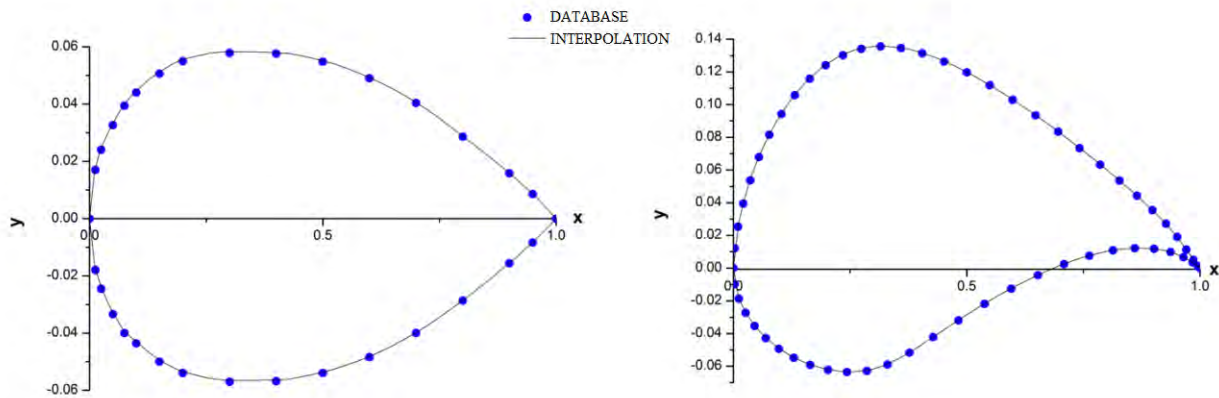


Figure 2. Examples of airfoils after interpolation of the database

In order to avoid the ANN to work at the saturation region, all the values were normalized so that they would be between -1 and 1. The normalization occurred by dividing each of the database values by their respective maximum value, which is 1.1401 for the Cl , 0.0282 for the Cd , 0.0923 for the Cm and 151,362 for the $Efmax$.

Aiming for a better use of the ANN work region (between -1 and 1), it was decided to modify the abscissa of the airfoil, which naturally possesses values between 0 and 1, so that it would fill the space between -1 and 1.

2.3 Network Architectures utilized

Two different types of network architectures were used in the modeling of the airfoils analyzed in this work: a multilayer perceptron network and a modular architecture. In both architectures, five input neurons and two output neurons were used. The aiming of this distribution was to obtain an input-output mapping to present the constants of the airfoil, as shown in Eq. 1

$$[ARQ \ ESP] = f(x, Cl, Cd, Cm, Efmax) \quad (1)$$

In Eq. 1, the variables ARQ and ESP respectively stand for curvature of the airfoil and thickness of the airfoil to each point in the x axis. The curvature, also known as mean camber, has its data collected in every point corresponding to its position in the horizontal axis. The thickness is the distance between the upper camber and the lower camber analyzed for every position of the horizontal axis (Raymer, 1992).

During the training, the cross-validation technique was applied, in which it is verified the value of the root-mean-square error (RMS) for the training and validation sets, selecting the synaptic weights with the lowest RMS for the validation set. In all situations, 2500 epochs were used, varying in number of hidden neurons between 5 and 30.

2.3.1 Multilayer Perceptron Networks (MLP)

A network is named perceptron when it has, as its main features, the utilization of non-linear models and a feedforward neural structure, proposed by McCulloch and Pitts (1943). From the data obtained by the preprocessing, the training of multilayer perceptron network architectures was executed. Due to the complexity of the proposed problem (obtainment of the airfoil from its characteristics), it was decided to test architectures with one (Fig. 3(a)) and two hidden layers (Fig. 3(b)). In both cases, six inputs (including the bias) and two outputs were used. Sigmoid functions were used in the hidden layers, and a linear function was used in the output layer. The **nor** sub index presented in the figures is referring to the normalized values. For the network training, the backpropagation algorithm was used, based on momentum.

A schematic diagram demonstrating the means of training of the ANN and the obtained model is shown in Fig. 4. In this figure, **TRE** represents the number of airfoils utilized for the ANN training, **TOD** the total number of airfoils utilized, e represents the error obtained between the desired response and the actual response of the ANN, and w , the matrix of synaptic weights of the ANN.

B. Diniz, R. Freire Júnior and S. de Souza
 Desenvolvimento de perfis aerodinâmicos a partir de suas características utilizando Redes Neurais Artificiais

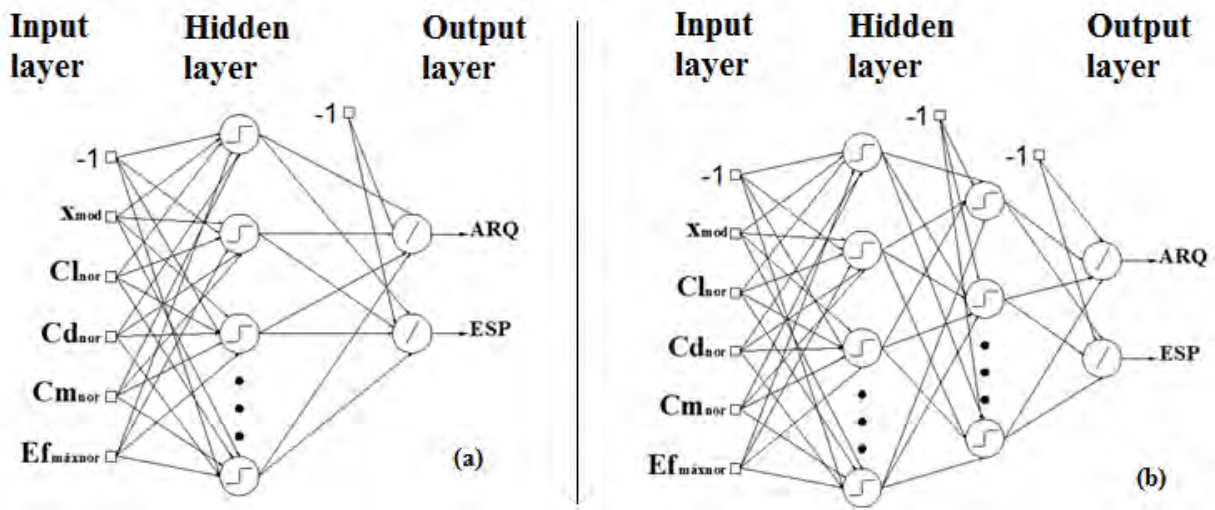


Figure 3. Perceptron network (a) with one hidden layer; (b) with two hidden layers

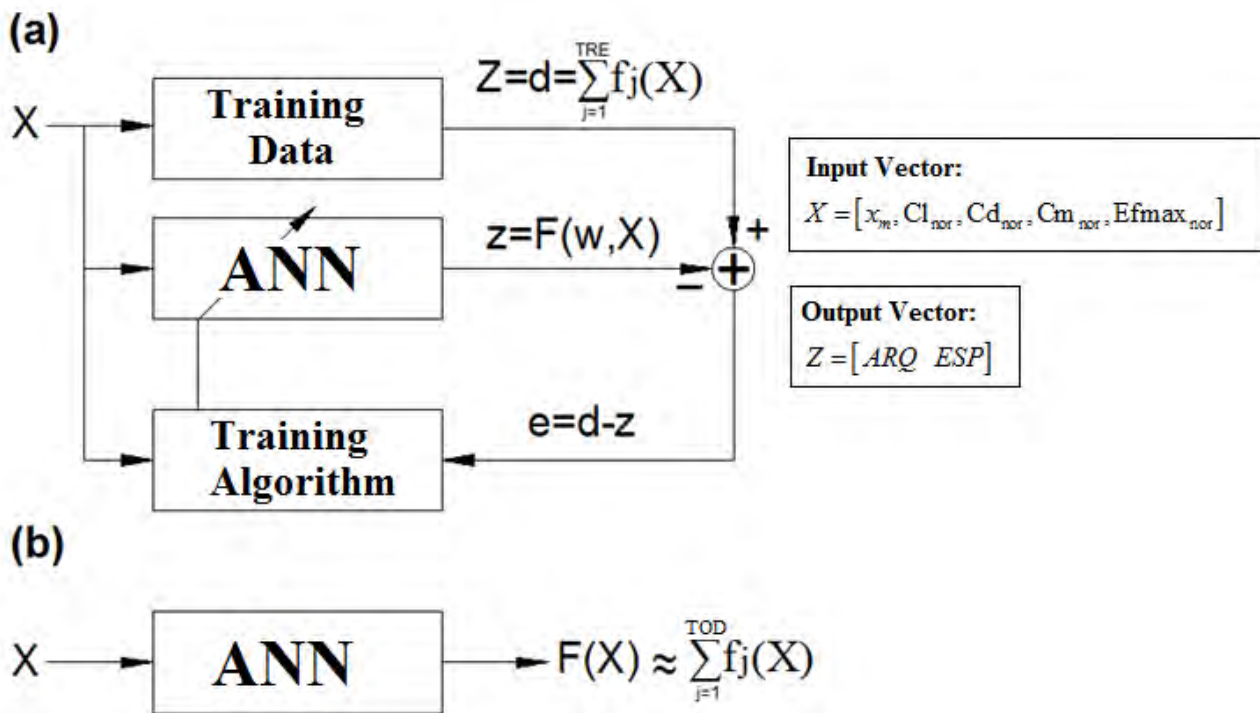


Figure 4. (a) ANN training method; (b) Model obtained from the ANN test

2.3.2 Modular Networks

One of the great advantages of the utilization of modular networks in the modeling of any physical behavior is the possibility of creating specialists through different training processes in each module. In this type of architecture, it is necessary to use the gating networks, which adds responsibilities to each module, making them accountable in larger or smaller scale for the general network result. Fig. 5 shows the behavior of the modular network applied to a general case (Haykin, 2001).

It is worth noting that each module used in the architectures proposed in this work represents a multilayer perceptron network with the same architecture presented in item 2.3.1. In order to proceed with the network training, architectures of two, three and four modules were used.

According to Jacobs *et al.* (1991), the partition in modules aims to divide the problem, making the modules become specialists in each airfoil region, for example, for a modular network with two modules, the first would specialize in presenting the geometry of the leading edge of the airfoil, whereas the second would specialize in the trailing edge of the airfoil. For a network with three modules, the first module would specialize in presenting the geometry of the

leading edge of the airfoil, the second would specialize in the middle section of the airfoil, whereas the third would specialize in the trailing edge of the airfoil.

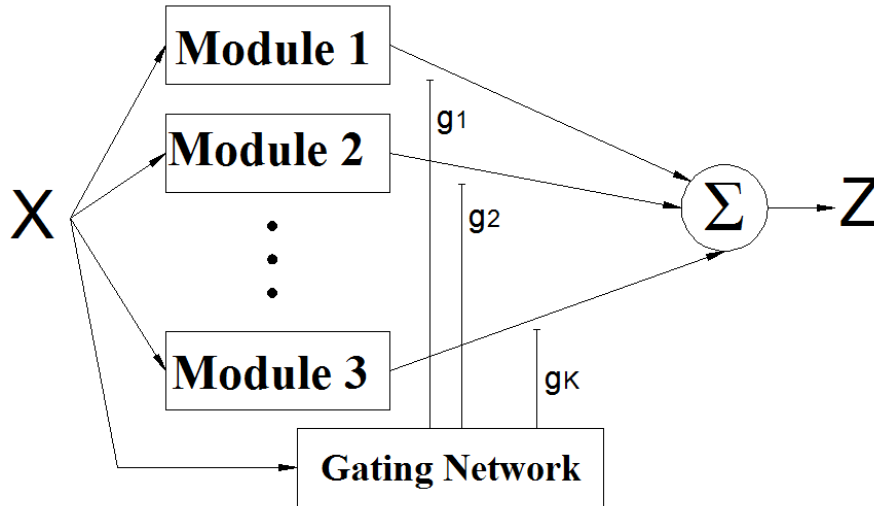


Figure 5. Modular network architecture

The equating utilized for the gating network determines the accountability attributed to each module in the architecture, depending on the airfoil region analyzed. For the simplification of intermediary equations, a rule was elaborated so that a number \mathbf{K} of modules could be applied to the network architecture, according to Eq. 2 (Freire Júnior, 2005).

$$g_k = \frac{1}{1 + e^{(B_k + A_k \cdot x_m)}} - \frac{C_k}{1 + e^{(D_k + A_k \cdot x_m)}} \quad (2)$$

In Eq. 2, B_K and D_K are constant positions, A_K is the slope parameter of the curve, C_K is the constant for the cancellation, or not, of the second term of the general equation, and g_K , which represents the gain of the gating network, of a total of \mathbf{K} modules. Aiming to better illustrate the problem, the gating networks curves (g) are traced as a function of x_m , as observed in Fig. 6.

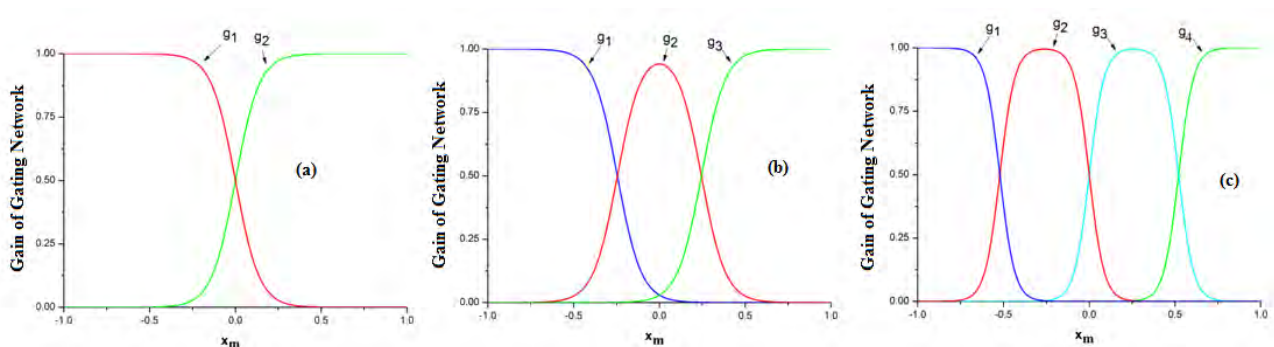


Figure 6. Curves of the gain of the gating networks with (a) two modules; (b) three modules; (c) four modules

The entire process executed in the development of this work is represented in the flowchart in Fig. 7, describing all steps for the accomplishment of this work.

B. Diniz, R. Freire Júnior and S. de Souza

Desenvolvimento de perfis aerodinâmicos a partir de suas características utilizando Redes Neurais Artificiais

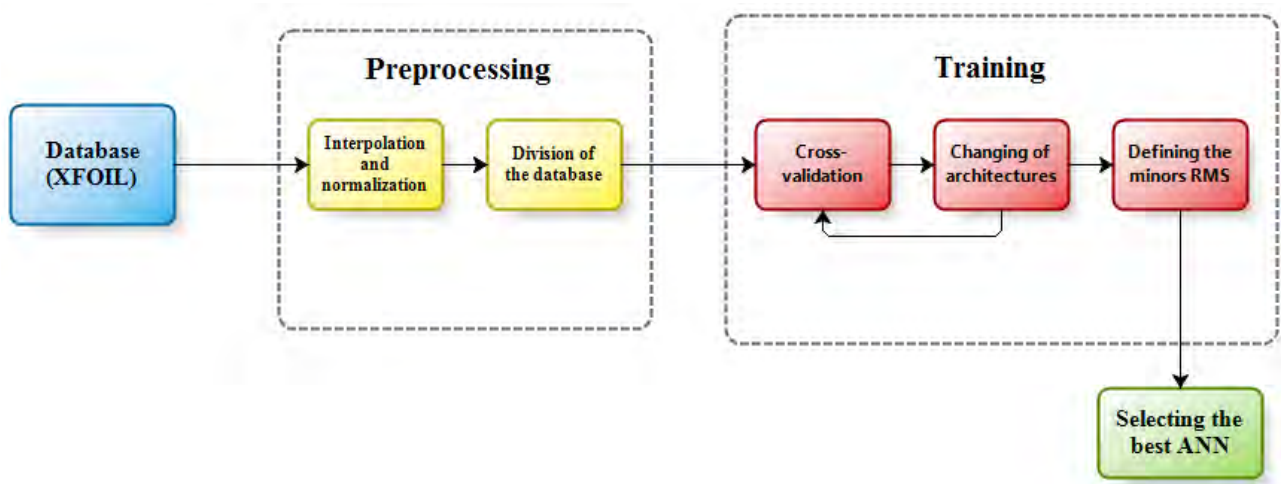


Figure 7. Flowchart of the methodology steps

3. RESULTS AND DISCUSSION

At first, different types of network architectures – of the perceptron type and the modular type - were used in the execution of the training of the collected database. All of the architectures that were trained and analyzed have five input neurons and two output neurons, and the cross-validation technique was applied, in which the value of the root-mean-square error (**RMS**) was verified in the training and validation sets, and the synaptic weights with the lowest **RMS** value were selected for the validation set.

The perceptron and modular network architectures are displayed in Tab. 2, and also the average **RMS** values for the validation and training sets, in a total of 300 airfoils.

Table 2. Perceptron and Modular architectures and their **RMS** values

ARCHITECTURE	HIDDEN LAYERS	RMS (TRAINING)	RMS (VALIDATION)
Perceptron network	1	19.36E-05	14.648E-05
Perceptron network	2	43.642E-05	113.7E-05
2 Modules	1	13.540E-05	5.6700E-05
2 Modules	2	9.944E-05	7.098E-05
3 Modules	1	12.526E-05	7.6050E-05
3 Modules	2	13.239E-05	9.723E-05
4 Modules	1	22.48E-05	62.94E-05
4 Modules	2	22.27E-05	10.98E-05

Another way to analyze the results in Tab. 2 is through Fig. 8, in which is noticed that the increase in the number of modules decreases the **RMS**, except for the case containing four modules.

The individual **RMS** for each airfoil is shown in Fig. 9 and 10, which have the **RMS** values in the vertical axis - and in the horizontal axis, the numbers corresponding to the airfoil analyzed. It is worth mentioning that the last thirty airfoils analyzed (270-300) belong to the test set, i.e., they were not utilized in cross-validation.

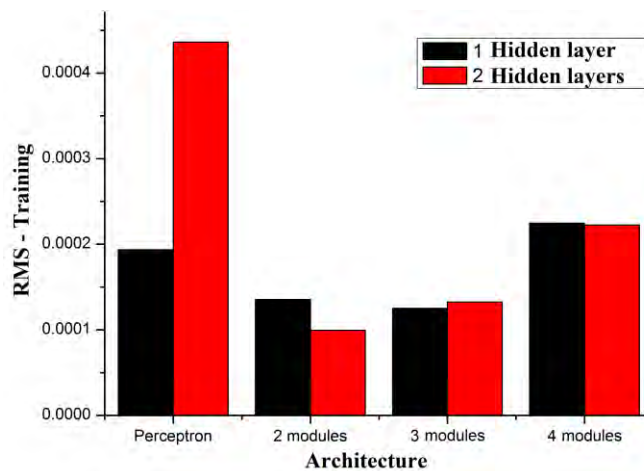


Figure 8. RMS vs. network architectures: the comparison between numbers of hidden layers

With the results presented in Fig. 9 and 10, it is noticed that the variation in the **RMS** presented a steady pattern of behavior for each analyzed airfoil, except for the perceptron architectures with two hidden layers, and the modular architectures with four modules (Fig. 10 (b)), which did not present satisfactory results, regardless of the analyzed airfoil.

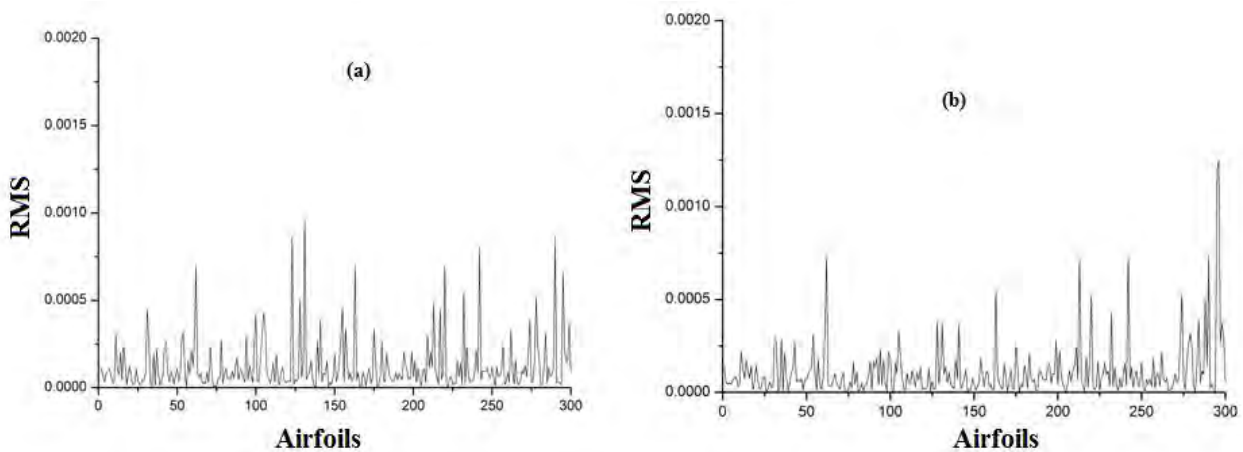


Figure 9. RMS vs. Airfoils – perceptron network (a) with one hidden layer (b) two-module network with two hidden layers

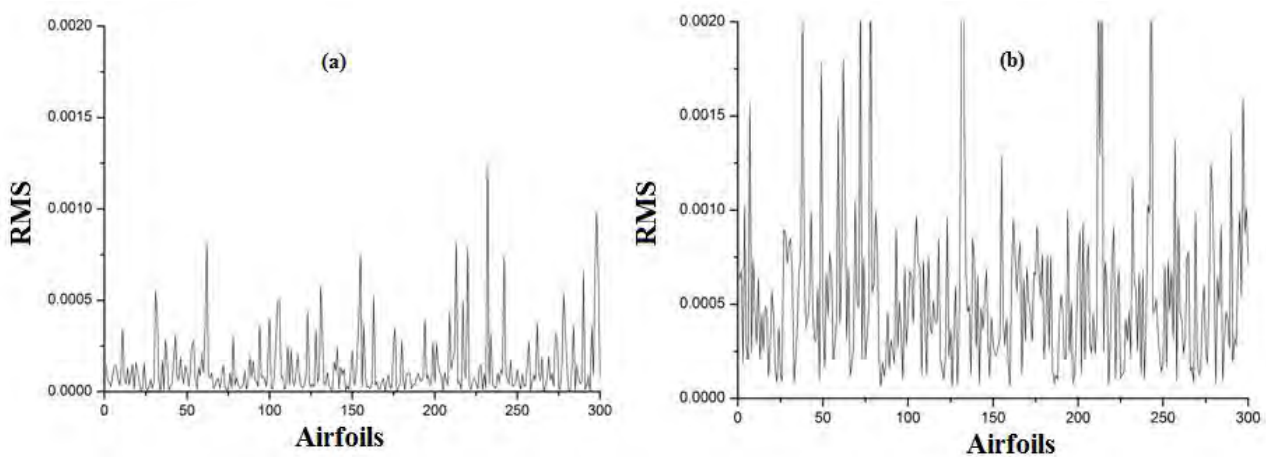


Figure 10. RMS vs. Airfoils – three-module network (a) with one hidden layer; (b) four-module network with one hidden layer

Considering now, more specifically, the architectures presenting very small errors in the largest possible number of airfoils evaluated, Tab. 3 was developed to present the number of airfoils in which the **RMS** was lower than 10^{-4} and 10^{-5} for each tested architecture. With these results, it is perceived that the architecture with two modules and two hidden layers presents the largest number of airfoils modeled with one small error, in which 197 airfoils were obtained with **RMS** lower than 10^{-4} and 21 airfoils with **RMS** lower than 10^{-5} .

Table 3. Amount of RMS values for each architecture

ARCHITECTURE	HIDDEN LAYERS	RMS	
		< E-04	< E-05
Perceptron network	1	197	12
Perceptron network	2	0	0
2 Modules	1	164	15
2 Modules	2	197	21
3 Modules	1	193	18
3 Modules	2	197	5
4 Modules	1	17	0
4 Modules	2	0	0

3.1 Evaluation of the test set for the two-module network with two layers of hidden neurons

According to the results presented in the preceding item, the modular architecture with the best result was the one with two modules and two layers of hidden neurons, in which the amount of neurons in the first layer was 30, and in the second layer was 13, for both modules.

It is necessary to perform a division of the entire database into a *training set* and a *validation set*. Besides this initial division, it might be necessary to create another database, the *test set*.

The test set, which represents an entirely new set to be presented to the network for performance evaluation, contains thirty values, as shown in section 2.2. In order to analyze this database, four airfoils from the test set with the lowest root-mean-square error values will be compared. The original airfoils compared to the obtained airfoils from the test set are represented in Fig. 11: NACA 0006, HQ 0-7, and Fig. 12: NACA 63209 and RAF 31.

In Fig. 11 and Fig. 12, it is possible to observe satisfactory results for the airfoils from the test set, when compared to the original dimensions of the airfoils, thus proving the efficiency of the learning algorithms utilized in the work.

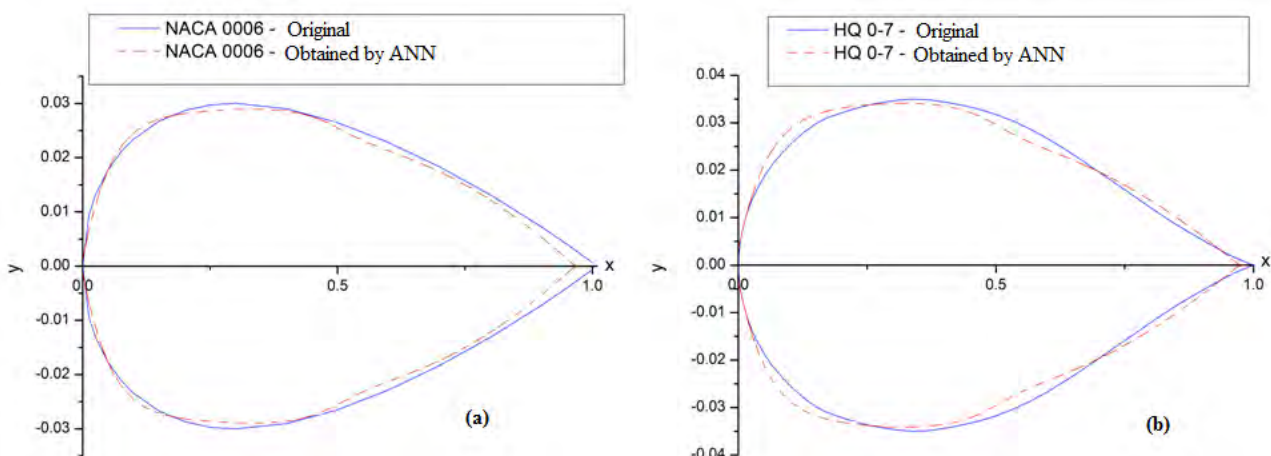


Figure 11. Original airfoil vs. Airfoil obtained by modular architecture: (a) NACA 0006; (b) HQ 0-7

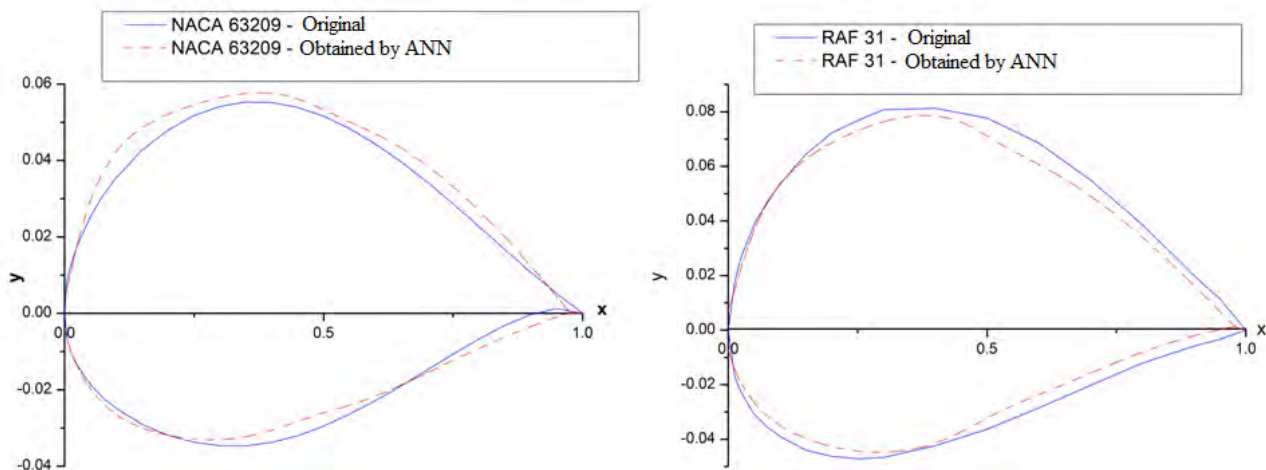


Figure 12. Original airfoil vs. Airfoil obtained by modular architecture: (a) NACA 63209; (b) RAF 31

3.2 Comparison between the results obtained by the modular network and the results obtained by XFOil

Considering the regions which presented results with the lowest **RMS** values in the graphs in Fig. 9(b) (region with C_l value between 0 and 0.25, C_d value between 0.007 and 0.02, C_m value between -0.05 and 0.01 and E_{fmax} between 40 and 70), four airfoils were developed through the **ANN**, represented as PRNA-1, PRNA-2, PRNA-3 and PRNA-4.

From the dimensions of the created airfoils, their geometry was imported to XFOil and the values of the aerodynamic coefficients were generated. Tab. 4 shows the images of the airfoils and the comparison between the analyzed parameters.

Tab. 4 exhibits two models for data presentation, the **ANN** model and the **XFOil** model. In the **ANN** model it is presented the aerodynamic characteristics that were utilized as inputs of the airfoil development function created in this work. In the **XFOil** model it is presented features generated by the software simulation after the import of the airfoils developed by the neural network. Therefore, it is possible to establish a comparison between the characteristics of both models.

In Tab. 4, it is possible to observe the proximity between the values obtained by the developed airfoils (PRNA) and the values obtained by the software. The largest differences between the data, in percentage, are found in the values of maximum efficiency rate for the PRNA-4 airfoil (20%), in the values of the drag coefficient for zero angle of attack in the PRNA-3 airfoil (15%) and in the PRNA-2 airfoil (10,5%), in the momentum values for zero angle of attack in the PRNA-3 airfoil (10%). The value in parenthesis in the maximum efficiency line of the XFOil model represents the angle of attack in which occurs the maximum efficiency value. Bearing in mind that the maximum efficiency rate is not related to the angle of attack, in opposition to the lift, drag and momentum coefficients.

Table 4. Comparison between the data obtained from the modular ANN and the data obtained from XFOil

Model	Features	Airfoil 1	Airfoil 2	Airfoil 3	Airfoil 4
		PRNA-1	PRNA-2	PRNA-3	PRNA-4
ANN	C_l	0.2	0.245	0.145	0
	C_d	0.0075	0.0095	0.0085	0.006
	C_m	-0.06	-0.039	-0.03	0
	E_{fmax}	47.5	70	50	50
XFOil	C_l	0.1991	0.236	0.1383	0.0065
	C_d	0.0069	0.0085	0.01	0.0073
	C_m	-0.052	-0.0418	-0.0273	-0.0002
	E_{fmax}	43.7	72.74	47.22	40

From these results, it is seen the possibility of applying an **ANN** in airfoil analysis, going away in the opposite direction from what is normally achieved by other software (XFOil, for instance), i.e., obtaining an airfoil from the desired aerodynamic characteristics.

4. CONCLUSIONS

The obtained results allow the following conclusions:

The learning algorithms utilized in this work were able to develop airfoils, obtaining satisfactory results when compared to the original airfoils. This fact was proved with the analysis of the data obtained by the test sets of the ANNs;

The network architectures with the lowest root-mean-square error values, therefore the best results, were the two-module network with two hidden neuron layers and the perceptron network with one hidden neuron layer, and the former presented more satisfactory results. This result was obtained when analyzing the amount of **RMSE** values below 10^{-4} and 10^{-5} (Tab. 3). The modular architecture obtained 21 values below 10^{-5} and 197 values below 10^{-4} .

Comparing the obtained airfoils from the test set (data which were not used during the ANN training) to the two-module network with two hidden layers, with the original airfoils, it is perceived a resemblance in the dimensions of the analyzed examples: NACA 0006 and HQ 0-7.

Analyzing the graph regions with the lowest **RMS** values in Fig. 9(b), airfoils were developed with characteristics based on such regions, and their geometries were imported to XFOIL, where new aerodynamic coefficients were generated and compared to the coefficients inserted in the network. Similar results were obtained between both data, as shown in Tab. 4.

5. BIBLIOGRAPHY

- DRELA, M. e YOUNGREN, H. (2001), *XFOIL 6.9 User Primer*, MIT Aero & Astro, 31p.
- EPPLER, R. *Direct Calculation of Airfoils from Pressure Distribution*. NASA TT F-15,417, 1974.
- FREIRE JÚNIOR, Raimundo Carlos Silvério. *Fadiga de Alto Ciclo em Compósitos de PRFV. Modelagem por RNAs e Prevenção de Falha*. 2005. Tese (Doutorado) - Universidade Federal do Rio Grande do Norte, Natal, 2005.
- HAYKIN, Simon. *Redes Neurais: Princípios e Prática*. 2^a ed.: Bookman, 2001. 893 p.
- JACOBS, R. A., JORDAN, M. I., BARTO, A. G.; *Task Decomposition Through Competition in a Modular Connectionist Architecture: The What and Where Vision Tasks*, *Cognitive Science*, Vol 15, pp. 219-250, 1991.
- MAEZABADI, Rasi F.; MASDARI, M.; SOLTANI, M. R. *Application of Artificial Neural Network for the Prediction of Pressure Distribution of a Plunging Airfoil*, The International Conference on Fluid Mechanics, Heat Transfer and Thermodynamics (FMHT2008). Paris, França, 2008.
- McCULLOCH, W. e PITTS, W. (1943). *A logical calculus of the ideas immanent in nervous activity*. *Bulletin of Mathematical Biophysics*, 7:115 - 133.
- NORGAARD, Magnus; ROSS, James C.; JORGENSEN, Charles C. *Neural Network Prediction of New Aircraft Design Coefficients*. NASA TM 112197, 1997.
- RAI, M. M.; MADAVAN, N. K. *Aerodynamic Design Using Neural Network*, *AIAA Journal*, Vol. 38, No. 1, pp 173-182, 2000.
- RAJKUMAR T.; BARDINA J. *Prediction of Aerodynamic Coefficients Using Neural Network for Sparse Data*. Proc. of FLAIRS 2002, Florida, EUA, 2002.
- RAJKUMAR T.; BARDINA J. *Training data requirement for a neural network to predict aerodynamic coefficients*. Proceedings of 17th Annual International Symposium on Aerospace/Defense Sensing, Simulation and Controls. Orlando, EUA, 2003.
- RAYMER, Daniel P. *Aircraft design: A Conceptual Approach*. Washington: AIAA, 1992.
- RODRIGUES, Luiz Eduardo M. J. *Fundamentos da engenharia aeronáutica: Aplicações ao Projeto SAE – AeroDesign*. São Paulo: Edição do Autor, 2010. cap. 2.
- ROSS, James C.; JORGENSEN, Charles C.; NORGAARD, Magnus. *Reducing Wind Tunnel Data Requirements Using Neural Networks*. NASA Technical Memorandum 112193, 1997.
- SOLTANI M. R.; GHORBANIAN K.; GHOLAMREZAEI M.; AMIRALAEI M. R. *Unsteady Three Dimensional Aerodynamic Load Prediction Using Neural Network*, IEEE International Joint Conference on Neural Networks, Orlando, EUA, 2007.
- TRUCKENBRODT, E. *Die Berechnung der Profilform bei vorgegebener Geschwindigkeitsverteilung (The Calculation of the Airfoil Shape from Specified Velocity Distribution)*. *Ingenieur-Archiv*, Bd. 19, Heft 6, 1951, pp. 365-377.
- WALLACH, R.; MATTOS, B. S.; GIRARDI, R. M.; CURVO, M. *Aerodynamic Coefficient Prediction of a General Transport Aircraft Using Neural Network*. In: 25th International Congress of the Aeronautical Sciences, 2006, Hamburgo, Alemanha. Proceedings of the 25th International Congress of the Aeronautical Sciences, 2006.
- WORTMANN, F. X. *Progress in the Design of Low Drag Aerofoils*. *Boundary Layer and Flow Control*, Volume 2, G. V. Lachmann, ed., Pergamon Press (London), 1961, pp. 748-770.